Vol. 83 (1993) *ACTA PHYSICA POLONICA A* No. 2

SPIN–LATTICE RELAXATION AND SUPERPOSITION MODEL CALCULATION IN Gd^{3+}-DOPED $LiErF_4$ AND $LiDyF_4$ CRYSTALS

L.E. MISIAK

Experimental Physics Department, M. Curie-Skłodowska University
Pl. M. Curie-Skłodowskiej 1, 20-031 Lublin, Poland

(Received May 21, 1992; revised version September 8, 1992)

The X-band EPR measurements were performed on Gd^{3+}-doped $LiErF_4$ and $LiDyF_4$ single crystals at room temperature. The spin–lattice relaxation times were evaluated to be 2.7×10^{-15} s, 1.0×10^{-15} s and 2.2×10^{-15} s for $LiDyF_4$, $LiErF_4$ and $LiYbF_4$, respectively. Spin-Hamiltonian parameters are determined and discussed in the light of the superposition model in order to determine the distortion of Gd^{3+} ion environment in $LiREF_4$ host lattices (RE = Yb, Y, Er, Dy, and Gd).

PACS numbers: 76.30.Kg

1. Introduction

$LiErF_4$ and $LiDyF_4$ crystals have been recently used as laser materials [1, 2]. Crystals of $LiREF_4$ (RE = rare earths) family were grown by Czochralski [3] and Bridgmann–Stockbarger methods [1]. The IR spectra in these crystals were also recorded [3]. The EPR of $LiREF_4$ and $LiY_{1-x}RE_xF_4$ (RE = Tb, Ho, Er) was carried out by Magarino et al. [4] and Tuchendler [5], respectively, using millimeter and submillimeter frequencies. The impurity resonances of Nd^{3+}, Dy^{3+}, Er^{3+}, and Yb^{3+} were investigated at X band in $LiYF_4$ single crystal [6]. The magnetic and NMR measurements of $LiErF_4$ and $LiHoF_4$ crystals were carried out by Hansen et al. [7]. Next, the NMR of fluorine and lithium nuclei in $LiREF_4$ (RE = Tb, Dy, Ho, Er) have been studied at 295 K [8].

The $LiREF_4$ crystals are magnetically concentrated crystals of relatively high symmetry (the point symmetry is S_4 — approximately D_{2d}). Further, these crystals are interesting because, although their structure is isomorphous to well-known scheelite ($CaWO_4$), they possess single F^- ions around an impurity ion compared to groups of ions in scheelites. The body-centered tetragonal crystal structure contains four magnetically equivalent RE^{3+} ions per unit cell. It is expected that trivalent Gd^{3+} ions substitute for trivalent RE^{3+} ions (RE = Er, Dy) without

charge compensation. By doping of $LiREF_4$ crystals with Gd^{3+} ions, the surrounding of the ionic impurity may be modified while preserving the local point symmetry of RE^{3+} ions. Therefore, $LiREF_4$ crystals were studied to interpret the spin-Hamiltonian parameters on the basis of the point-charge or the superposition model. From the theoretical standpoint the most useful ones are systematic EPR experimental data of the impurity Gd^{3+} ion in isostructural host lattices of rare-earth compounds. The main problem is to determine the exact local environment of the impurity centers in crystals. The local distortions caused by an impurity ion in the crystal lattices are generally unknown making a difficulty in the interpretation of EPR experimental data. The superposition model is useful when the ligands around an impurity ion are single ions, or small complex groups of ions.

The rare earths being ionic atoms are coupled predominantly by a dipole--dipole interaction, causing that EPR lines become broad. The $LiREF_4$ crystals are studied in order to compare their spin–lattice relaxation times dependent on a different strength of dipolar interactions. Spin–lattice relaxation times can be determined using experimental linewidths and taking into account the presence of two active ions (Gd^{3+} and RE^{3+}).

The paper deals with two separate problems: the spin–lattice relaxation and the calculation of a local distortion using the superposition model.

2. Crystal growth and crystal structure

$LiErF_4$ and $LiDyF_4$ (LEF and LDF, hereafter) crystals belong to the family of scheelite-type structure with the space group classification $I4_1/a$ (C_{4h}^6), likewise as $LiYF_4$ and $LiYbF_4$ [9, 10, 11].

LEF and LDF single crystals were obtained by the modified Bridgmann--Stockbarger method using an induction furnace and a resistance furnace. The technology of crystal growth in the induction furnace can be found elsewhere [12]. The components used for crystallization were: ErF_3, or DyF_3 (99.9% purity) and LiF (99.5% purity). The crystal growth was carried out in the resistance furnace controlled to $\pm 0.5°C$. The synthesis and the homogenization of mixture were performed at $\approx 1050°C$. The temperature at least 50–100°C higher than a melting point of a particular compound was used for crystal growth. A crucible was lowered with the rate of 1 mm/h through a freezing region, where the temperature gradient was 60°C/cm.

Crystals prepared for EPR experiment are generally of spherical shape, transparent light pink (LEF) and light yellow (LDF). The X-ray diffraction for $LiREF_4$ crystals was used to compare their structure and cell dimensions with those of given in references and to select more perfect samples.

The X-ray powder diffraction patterns of Cu K_α X-ray radiation ($\lambda = 0.15418$ nm) were recorded on crushed material. The spectra were analyzed using computer programs in order to find Miller indices and to calculate lattice constants. The presently determined lattice constants at room temperature for $LiErF_4$ ($a = 0.5150 \pm 0.0008$ nm, $c = 1.070 \pm 0.001$ nm) and for $LiDyF_4$ ($a = 0.5184 \pm 0.0008$ nm, $c = 1.083 \pm 0.001$ nm) correspond to the published data as follows: for $LiErF_4$ —

$a = 0.5162 \pm 0.0005$, 0.516, and 0.515 nm, $c = 1.070 \pm 0.001$, 1.070, and 1.068 nm, for $LiDyF_4$ — $a = 0.5188 \pm 0.0005$, 0.519, and 0.5185 nm, $c = 1.083 \pm 0.001$, 1.081, and 1.084 nm in Refs. [9], [13], and [3], respectively.

3. Experimental details

EPR of Gd^{3+} ions was carried out at X band in LEF and LDF single crystals. The EPR experimental arrangement has been described elsewhere [14].

4. Spin–lattice relaxation time (SLRT)

The measurements indicate broadening of the EPR lines with the decrease in temperature. This fact can be attributed to a slowing down of the relaxation rate in the rare-earth spin system, starting at rather high temperatures because of the absence of strong exchange interactions in these systems. The width of broad lines (Fig. 1) is in the range 75–86 mT at room temperature. The lines have

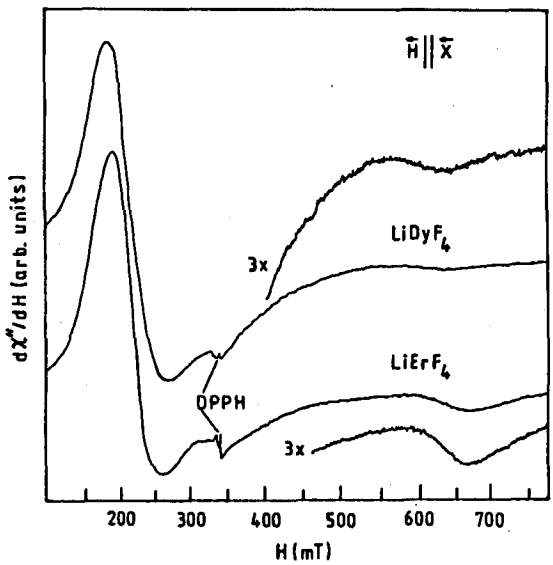

Fig. 1. EPR spectra of Gd^{3+}-doped $LiREF_4$ (RE = Er, Dy) crystals at room temperature ($\boldsymbol{H} \parallel \boldsymbol{X}$).

a Lorentzian shape due to a narrowing mechanism which influences the dipolar interaction between Gd^{3+} and Er^{3+} (or Dy^{3+}) spins. The magnetic moments of Er^{3+} ($9.5\mu_B$) and Dy^{3+} ($10.6\mu_B$) are larger than the magnetic moment of Yb^{3+} ($4.5\mu_B$) in consistence with the observed linewidths in $LiREF_4$ crystals.

In the theory of Van Vleck the impurity and the host ions Lande factors (g, g') are assumed to be different, therefore the resonance lines of impurity and host ions do not overlap [15]. The broadening taken into consideration is caused

essentially by the magnetostatic interaction of the atomic dipoles, and is hence "adiabatic" in character. Van Vleck assumed that the moments responsible for the absorption are magnetic, and arise from nuclear or electronic spins (from two electronic spins in Gd^{3+}-doped $LiREF_4$). The influence of the crystalline electric field is neglected and the material is supposed to be non-ferromagnetic. (In $LiREF_4$ crystals all these conditions are fulfilled.) The usual assumption is that the resonance frequencies have a Gaussian distribution which is a good approximation for the dipolar interaction alone.

The expression is finally obtained for the mean square power frequency deviation in case of two spins present in crystal

$$\langle\overline{\Delta\nu^2}\rangle = \frac{1}{3}S(S+1)h^{-2}\sum_k B_{jk}^2 + \frac{1}{3}S'(S'+1)h^{-2}\sum_{k'} C_{jk'}^2, \tag{1}$$

where B_{jk} and $C_{jk'}$ are defined as follows:

$$B_{jk} = -\frac{3}{2}g^2\mu_B^2 r_{jk}^{-3}\left(3\gamma_{jk}^2 - 1\right), \quad C_{jk'} = \tilde{A}_{jk'} + \left(1 - 3\gamma_{jk'}^2\right) gg'\mu_B^2 r_{jk'}^{-3}. \tag{2}$$

The symbol $\tilde{A}_{jk'}$ describes the effect of exchange interactions: e.g. if each ion has Z electrons in $4f$ shell, then $\tilde{A}_{jk} = -2Z^2 J_{jk}$, where J_{jk} is the usual exchange integral. The primed and the unprimed letters are used to distinguish two types of ions; the unprimed component is responsible for the resonance. The exchange interaction between similar ions does not appear in the expression for the second moment [15].

The first term of Eq. (1) represents the dipolar contribution from the similar (unprimed) ions and can be neglected compared to the second term because of large distances between impurity ions. The distance in the first term of Eq. (1) appears to be to the inverse sixth power. The concentration of Gd atoms in LEF and LDF crystals is 0.2 mol%, therefore the probability of dipolar interaction between Gd^{3+} ions is small, because each Gd^{3+} ion in LEF and LDF is surrounded by paramagnetic RE^{3+} ions. The concentration of impurity atoms doped to crystals used in EPR experiments (e.g. in $LiREF_4$) is usually from 0.1 to 0.5 mol%. The dipolar interactions between Gd^{3+} and RE^{3+} ions contribute to the second term of Eq. (1).

The full width at half peak of a Gaussian distribution is given by the expression [15, 16]:

$$\Delta H_{\text{dip-ex}}^2 = (2.35)^2 h^2 \langle\overline{\Delta\nu^2}\rangle / g^2\mu_B^2. \tag{3}$$

According to Mitsuma [17] the relaxation processes of the host ions modulate the dipolar and exchange interactions between the host (RE^{3+}) and the impurity (Gd^{3+}) ions causing that EPR impurity line becomes narrow. The spin–lattice relaxation is temperature dependent, whereas the exchange interactions are not. EPR lines broaden with lowering temperature, because τ_1' (the host SLRT) increases at low temperatures, thereby influencing more strongly the impurity ion linewidths due to enhanced dipolar interactions. Impurity ions have longer SLRT than host ions. The large effect of the host ions Er^{3+} (or Dy^{3+}) in Gd^{3+} spectra will be observed if SLRT of host ions approaches to SLRT of impurity Gd^{3+} ions [18]. This process produces an extra path for rapid transfer of energy to lattice.

The theory [17, 19] requires the fulfillment of the four conditions (fulfilled in $LiREF_4$ crystals) for the spin–lattice narrowing to be effective; then a Gd^{3+} linewidth at a half height of absorption line [17] can be expressed as follows:

$$\Delta H_{1/2} = \frac{20}{3}\Delta H^2_{\text{dip-ex}}/H_{\text{mod}}, \tag{4}$$

where $H_{\text{mod}} = h/g'\mu_B\tau_1'$.

The combination of (1), (2), (3), and (4) gives the proper equation to calculate SLRT of host ions (for an external magnetic field being along z axis) [15, 20]:

$$\tau_1' = \frac{1}{110.45g'S'(S'+1)}$$

$$\times \frac{9g^2\mu_B h f \Delta H_{\text{pp}}}{\left[NA_P^2 + G^2\sum_{k'}^{N}(1-3\gamma_{jk'}^2)^2 r_{jk'}^{-6} + 2A_P G\sum_{k'}^{N}(1-3\gamma_{jk'}^2)r_{jk'}^{-3}\right]}, \tag{5}$$

where the primed components are used for host ions, whereas the unprimed ones for impurity ions, $G = gg'\mu_B^2\mu_0$, S and S' are effective spins, $r_{jk'}$ are distances between the j and k' ions, $\gamma_{jk'}$ are direction cosines of $r_{jk'}$ with respect to an external magnetic field, $A_P = Z_1Z_2J_P = (0.53$ GHz) is the average host–impurity pair exchange integral $-2J_{jk'}$. (The total exchange integral for LEF and LDF [7] are experimentally determined to be in agreement with 4.2 ± 4.2 GHz for $LiTbF_4$ [21].) N (= 8) is a number of nearest and next-nearest neighbors taken into consideration, and ΔH_{pp} is an experimental value of the EPR peak-to-peak linewidth. f is the factor equal to 1.73 and 1.18 for Lorentzian and Gaussian lineshapes, respectively.

A calculation of τ_1' using (5) requires very precise crystal-structure data. Figure 2 shows nearest ($k' = 1$–4) and next-nearest ($k' = 5$–8) neighbor RE^{3+} ions of an impurity Gd^{3+} ion. The distances from Gd^{3+} to 1–4 nearest (r_1) and to 5–8 next-nearest (r_2) neighbor RE^{3+} ions are 0.3717 and 0.5160 nm for LEF, and 0.3747 and 0.5190 nm for LDF. The value of g' is equal to 3.137 and 1.112 for Er^{3+} and Dy^{3+} in $LiYF_4$ [6], respectively. The value of g can be found for Gd^{3+}-doped LEF and LDF in Table I and for $LiYbF_4(Gd^{3+})$ in [14]. The energy levels are: for $^4I_{15/2}$ ground term of Er^{3+} at 0, 27, 44, 95, 452, 517, 572, and 613 cm^{-1} in $LiErF_4$ [7] and for $^6H_{15/2}$ ground term of Dy^{3+} at 0, 42.3, 61.8, 110.9, 154.9, 210.7, 272.3, and 468.5 cm^{-1} in DyF_3 [22]. These levels were used to evaluate effective spins S' (= 7/2 for Er^{3+} and 9/2 for Dy^{3+}) assuming that effective spins are related to the highest energy level for which the Boltzmann distribution of population is in excess of 10%. The Yb^{3+} doublets of $^2F_{7/2}$ ground term in $LiYbF_4$ crystal are at 0, 235, 366, and 456 cm^{-1} [23]. SLRT's calculated from Eq. (5) are $(2.7 \pm 0.3) \times 10^{-15}$ s, $(1.0 \pm 0.3) \times 10^{-15}$ s, and $(2.2 \pm 0.2) \times 10^{-15}$ s using the room-temperature linewidths of 86(±5) mT, 82(±5), and 24.5(±1.5) mT (transition of $5/2 \leftrightarrow 3/2$; $\boldsymbol{H} \parallel z$) for LDF, LEF, and $LiYbF_4$ [20], respectively.

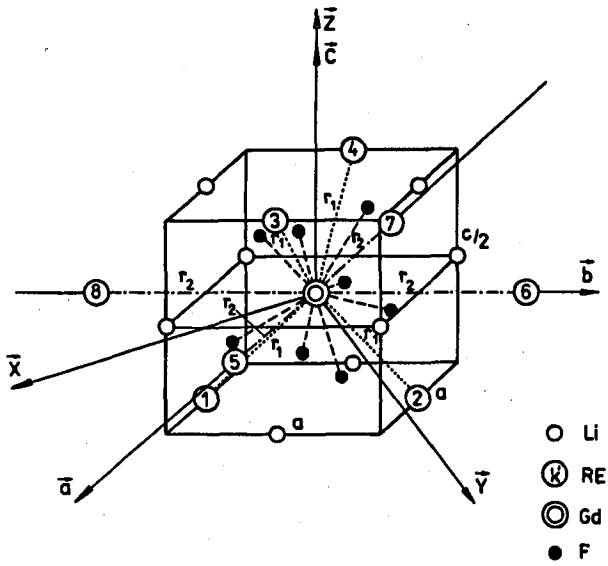

Fig. 2. The configuration of four nearest ($k' = 1$ to 4) and four next-nearest ($k' = 5$ to 8) neighbor RE^{3+} ions around the impurity Gd^{3+} ion in a half-unit cell of $LiREF_4$ crystal (RE = Er, Dy). For k' definition see Eq. (5).

5. Spin-Hamiltonian parameters and superposition model calculations

Angular variations of EPR lines for Gd^{3+}-doped $LiREF_4$ crystals in zx plane (Fig. 3) at room temperature are similar to those of $LiY_{1-x}Yb_xF_4(Gd^{3+})$ [14, 24], however, because of broad lines in the former, the spin Hamiltonian parameters are determined with greater errors than in the latter. The spin Hamiltonian was used to be the same as in Ref. [14]; the fitted values of spin-Hamiltonian parameters are presented in Table I.

The z axis coincides with the [001] crystal axis; the spectrum recorded for an external magnetic field along z axis shows the maximal overall splitting in the external magnetic field. The x and y axes are assumed to be in the plane perpendicular to the z axis in correspondence to equivalent positions of the maximal overall splitting in the xy plane (see angular variation in the xy plane [24]). On the other hand, assuming the x and y axes considered positions of the minimal overall splitting in the xy plane [24] and fitting the experimental data in the $zx_{\min}$ plane, the same absolute values (in error bars), but the opposite signs should be obtained only for b_4^4 and b_6^4 spin-Hamiltonian parameters [25], as compared to parameters obtained from the fitting of the experimental data in the $zx_{\max}$ plane; e.g., from the experimental data measured in the $zx_{\min}$ plane for $LiErF_4$ one evaluated $b_4^4 = -0.45 \pm 0.14$ and $b_6^4 = 0.40 \pm 0.19$ GHz ($\chi^2 = 4.4$ GHz^2). The parameters exhibited in Table I are evaluated using the experimental data measured in the $zx_{\max}$ plane.

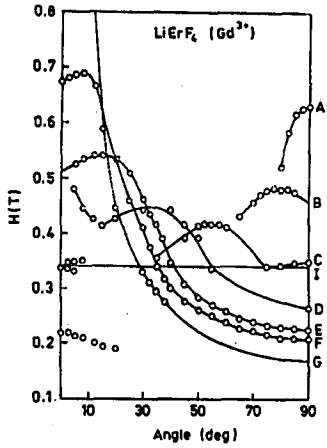

Fig. 3. Angular variation of the EPR line positions for Gd^{3+}-doped $LiErF_4$ single crystal in the zx_{max} plane at room temperature. The various transitions ($M \leftrightarrow M-1$) have been indicated as follows: $A(-5/2 \leftrightarrow -7/2)$, $B(-3/2 \leftrightarrow -5/2)$, $C(-1/2 \leftrightarrow -3/2)$, $D(1/2 \leftrightarrow -1/2)$, $E(3/2 \leftrightarrow 1/2)$, $F(5/2 \leftrightarrow 3/2)$, $G(7/2 \leftrightarrow 5/2)$, I(DPPH). The continuous lines connect data points belonging to the same transitions.

TABLE I

The values of the spin-Hamiltonian parameters for Gd^{3+}-doped $LiREF_4$ crystals (RE = Er, Dy) at room temperature. The b_n^m parameters are expressed in GHz, $\bar{N}$ represents a total number of line positions simultaneously fitted, and χ^2 is expressed in GHz^2. The measurements (in the zx_{max} plane) were performed for the x axis oriented in such a direction for which the maximum of overall splitting in the xy plane was observed.

	$LiErF_4$	$LiDyF_4$
g_{zz}	1.934 ± 0.042	1.923 ± 0.042
g_{xx}	2.016 ± 0.042	2.018 ± 0.042
b_2^0	-2.331 ± 0.053	-2.325 ± 0.061
b_4^0	-0.037 ± 0.022	-0.055 ± 0.025
b_4^4	0.256 ± 0.081	0.182 ± 0.074
b_6^0	-0.024 ± 0.025	-0.010 ± 0.033
b_6^4	-0.026 ± 0.150	-0.013 ± 0.172
$\bar{N}$	81	75
χ^2	3.8	3.4

TABLE II

The structural data of $LiREF_4$ crystals determined from the data given in the literature. The asterisk for b_2^0 of $LiGdF_4$ marks the extrapolated value. Dimensionless coordination factors a_d and b_d are calculated using θ_1 and θ_2 for a distorted host lattice. For the definition of symbols see Ref. [14].

	$LiYbF_4$	$LiErF_4$	$LiYF_4$	$LiDyF_4$	$LiTbF_4$	$LiGdF_4$
radius of RE^{3+} [nm]	0.0858	0.0881	0.0896	0.0908	0.0923	0.0938
c/a	2.063	2.074	2.078	2.088	2.095	2.102
R_1 [nm]	0.2218	0.2231	0.2246	0.2249	0.2253	0.2267
θ_1 [deg]	67°07′	67°00′	67°05′	66°50′	66°46′	66°40′
ϕ_1 [deg]	−32°58′	–	−33°00′	–	–	–
χ_1 [deg]	1°42′	–	1°30′	–	–	–
R_2 [nm]	0.2269	0.2288	0.2293	0.2313	0.2321	0.2339
θ_2 [deg]	141°52′	142°01′	142°03′	142°14′	142°22′	142°28′
ϕ_2 [deg]	−37°29′	–	−36°59′	–	−53°37′	–
χ_2 [deg]	−2°49′	–	−2°29′	–	–	–
R_0 [nm]	0.2244	0.2260	0.2270	0.2278	0.2287	0.2298
b_2^0 [GHz]	−2.4812	−2.331	−2.4863	−2.325	–	−2.210*
a	−1.0928	−1.0844	−1.0900	−1.0740	–	−1.0632
a_d	−0.5106	−0.9289	−0.6412	−0.9971	–	−1.0632
b	1.7122	1.7274	1.7310	1.7462	–	1.7655
b_d	0.9860	1.5226	1.1622	1.6443	–	1.7655
c	−0.3680	−0.3814	−0.3720	−0.3982	–	–
d	−1.0817	−1.0648	−1.0610	−1.0435	–	–
e	12.5190	12.4781	12.5260	12.4271	–	–
f	2.4953	2.4623	2.4660	2.4218	–	–

In order to understand the nature of crystalline field in scheelite crystals and the deformation due to introduction of Gd^{3+} ion into a host lattice, it is necessary to analyze the obtained data using, e.g., a point-charge or a superposition model. The point-charge model gives for $LiYF_4(Gd^{3+})$ the value of $b_2^0 \approx 6.1457$ GHz [26] which is 2.5 times greater than the experimental b_2^0 value and has the reverse sign. On the other hand, the calculation following the superposition model requires the exact crystal structure data, i.e., the exact knowledge of ligand positions F^- around a rare-earth ion and the lattice distortion produced by the substitution for smaller host lattice ions (Yb, Y, Er, Dy) by larger Gd^{3+} ions. The crystal structure parameters were calculated (see Table II) using lattice constants available in the literature (for $LiYF_4$ and partly for $LiYbF_4$ these parameters are in [27]). In order

to check the error in the calculation of the crystal data from lattice constants, for example, the calculated R_2 and θ_2 are compared with the experimental data determined by Als-Nielsen et al. [28] for $LiTbF_4$ crystal, being only different by 0.2 and 0.05%, respectively.

For more details of a superposition-model calculation see Refs. [14] and [24]. The intrinsic $\bar{b}_4$ and $\bar{b}'_4$ parameters evaluated from the experimental values of b_4^0 and b_4^4, respectively, are expected to be equal according to the superposition model. The analysis of spin-Hamiltonian parameters for LEF and LDF (using superposition model) gives the discrepancy between $\bar{b}_4$ and $\bar{b}'_4$ values ($\bar{b}_4 > \bar{b}'_4$) and both the same signs. (The agreement of signs is not always hold, e.g. for scheelites [26].) This discrepancy between $\bar{b}_4$ and $\bar{b}'_4$ can be explained by the local distortion around impurity Gd^{3+} ion. The available crystallographic data for pure crystals (obtained from neutron or X-ray diffraction), which are used to calculate the $\bar{b}_4$ and $\bar{b}'_4$, are distinct from the experimental crystal structure data because of the difference between Gd^{3+} and RE^{3+} ionic radii. The $\bar{b}_4$ and $\bar{b}'_4$ parameters are not equal to each other for t_4 values in the range within ± 20 (see Ref. [24]). Further, the decrease in θ_1 and θ_2 vertical angles by 1° results in the decrease in $\bar{b}_4$ by 16% while $\bar{b}'_4$ is practically constant [26]. It is assumed that the local distortion around an impurity ion may explain the discrepancy between $\bar{b}_4$ and $\bar{b}'_4$. In order to confirm this assumption it seems helpful to study spin-Hamiltonian parameters of the other members of $LiREF_4$ family.

The value of t_4 (≈ -60) calculated for considered crystals without taking into account any distortion is too large. Further, it is possible to evaluate the change ($\Delta\theta_1 = \Delta\theta_2 = \Delta\theta_{RE}$) of eight vertical angles θ_1^i and θ_2^{i+4} ($i = 1$ to 4) for F^- ions placed around RE^{3+} ion. In order to determine $\Delta\theta_{RE}$, the t_4 ($= -9$) is assumed for all $LiREF_4$ crystals. This mean value of t_4 is determined from stress experiments in $MeF_2(Gd^{3+})$ (Me = Cd, Ca, Sr, Pb, and Ba) crystals [29], where the local environment is similar to those in $LiREF_4$. The difference between the ionic radii of Gd^{3+} and Er^{3+} is 0.0057 nm. One can compute that if the RE^{3+}–F^- distances increase by about 0.006 nm, then t_4 parameter is changed by 2.6%. The value of t_4 increases by 50% for $R_1 \equiv R_1 - 0.003$ nm and $R_2 \equiv R_2 + 0.003$ nm, however, such a distortion is impossible in case of the substitution of a great Gd^{3+} ion for a small rare-earth host lattice ion. For considered local symmetry there are used (in the superposition-model calculations) χ_1 and χ_2 angles (equal to a few degrees) instead of ϕ_1 and ϕ_2 horizontal angles. The maximal increase in the χ_1 absolute value by 0.5° and in χ_2 by 1° changes t_4 by 5%. The similar situation takes place for the t_2 parameter which is mainly influenced by the change of θ_1 and θ_2, because the increase in both R_1 and R_2 by $r_{Gd} - r_{Dy} = 0.003$ and $r_{Gd} - r_{Yb} = 0.008$ nm changes the parameter t_2 maximally by 0.5 and 1.3%, respectively. The conclusion from the above discussion is following: it is sufficient to consider the prevailing part of distortion produced by the decrease in θ_1 and θ_2 vertical angles. The determined (from the superposition model) decreases in vertical angles θ_1 and θ_2 of eight fluorines around Gd^{3+} ion are as follows: $\Delta\theta_{RE} = 7.5°$, 5.5°, 2°, and 1° for RE = Yb, Y, Er, and Dy, respectively. The values of $\Delta\theta_{Yb} = 7.5°$ and $\Delta\theta_Y = 5.5°$ are determined more exactly because of the smaller errors of the experimental spin-Hamiltonian parameters.

TABLE III

The calculated values of $\bar{b}_2(R_0)$ for $LiREF_4$ crystals in case of the undistorted (upper value) and the distorted (lower value) host lattice. The distortion of $\theta_1^i \equiv \theta_1 - \Delta\theta_{RE}$ and $\theta_2^{i+4} \equiv \theta_2 - \Delta\theta_{RE}$ ($i = 1$ to 4 for fluorine ions) is introduced using the evaluated values of $\Delta\theta_{Yb} = 7.5°$, $\Delta\theta_Y = 5.5°$, $\Delta\theta_{Er} = 2°$, $\Delta\theta_{Dy} = 1°$, and $\Delta\theta_{Gd} = 0°$.

t_2	$LiYbF_4$	$LiErF_4$	$LiYF_4$	$LiDyF_4$	$LiGdF_4$
−6	−3.0557	−2.7209	−3.0419	−2.5464	−2.2760
	−4.2948	−2.9895	−3.9272	−2.6667	–
−4	−3.3196	−2.9694	−3.2789	−2.7939	−2.5096
	−4.5660	−3.2494	−4.1750	−2.9194	–
−2	−3.6315	−3.2657	−3.5544	−3.0922	−2.7936
	−4.8715	−3.5568	−4.4544	−3.2223	–
0	−4.0058	−3.6256	−3.8788	−3.4591	−3.1468
	−5.2184	−3.9261	−4.7721	−3.5925	–
1	−4.2226	−3.8362	−4.0635	−3.6761	−3.3579
	−5.4101	−4.1402	−4.9479	−3.8102	–
2	−4.4636	−4.0721	−4.2663	−3.9215	−3.5985
	−5.6158	−4.3785	−5.1366	−4.0552	–
3	−4.7333	−4.3383	−4.4899	−4.2011	−3.8753
	−5.8372	−4.6452	−5.3400	−4.3331	–
4	−5.0370	−4.6412	−4.7378	−4.5229	−4.1971
	−6.0760	−4.9459	−5.5594	−4.6509	–
5	−5.3816	−4.9888	−5.0140	−4.8972	−4.5762
	−6.3345	−5.2875	−5.7972	−5.0181	–
6	−5.7760	−5.3920	−5.3239	−5.3380	−5.0292
	−6.6152	−5.6791	−6.0558	−5.4471	–
7	−6.2321	−5.8652	−5.6740	−5.8650	−5.5805
	−6.9212	−6.1326	−6.3379	−5.9551	–
8	−6.7655	−6.4287	−6.0728	−6.5062	−6.2659
	−7.2562	−6.6641	−6.6470	−6.5663	–
9	−7.3978	−7.1110	−6.5312	−7.3036	−7.1416
	−7.6244	−7.2955	−6.9873	−7.3160	–
10	−8.1595	−7.9543	−7.0636	−8.3222	−8.2997
	−8.0311	−8.0581	−7.3637	−8.2572	–

Table III shows the calculated values of the $\bar{b}_2(R_0)$ parameters in the case of undistorted and distorted environment of Gd^{3+} ion. The decrease in $\bar{b}_2$ absolute values for $LiREF_4(Gd^{3+})$ along the rare-earth series relates to the decrease in their differences between Gd^{3+} and RE^{3+} ionic radii. The values of $\bar{b}_2(R_0)$ are more consistent for $t_2 = 5.5$ and 8 in the case of undistorted and distorted lattice, respectively. These t_2 values can be compared with those of assumed by Newman and Urban [30] ($t_2 = 1$) accounted for cancellation effects, and by Vishwamittar and Puri [31] ($t_2 = 2.5$) for scheelite-type crystals $MeWO_4$, $MeMoO_4$ (Me = Ca, Sr, Ba, Pb). The values of b_2^0 in $MeWO_4$ and $MeMoO_4$ are almost the same as in $LiREF_4(Gd^{3+})$ but environments of RE^{3+} ions are different. Newman and Urban [30] have determined for scheelite $MeWO_4$ and $MeMoO_4$ crystals the $\bar{b}_2(0)$ values in the range from -6.3 to -5.6 GHz which are consistent with those of calculated presently for $t_2 = 7$ (see Table III). On the other hand, the values of $\bar{b}_2(R_0)$ for $REF_3(Gd^{3+})$ (RE = La, Ce, Pr, Nd) [32], are in the range from -5.3 to -4.5 GHz, whereas b_2^0 parameters are in the range of 0.7–0.8 GHz. The value $t_2 = 8 \pm 1$ is determined for Fe^{3+} ion substituted for Ti^{4+} in $BaTiO_3$ using the superposition-model analysis [33].

In addition, in order to determine the t_2 parameter, $b_2^0 = -2.210$ GHz for $LiGdF_4$ was extrapolated from the linear dependence of b_2^0 on the difference between Gd^{3+} and RE^{3+} ionic radii [34] for $LiYbF_4$, LEF, and LDF crystals. A Gd^{3+} ion in $LiGdF_4$ is in undistorted environment, whereas in $LiREF_4$ crystals there are some distortions. Using the superposition model [32] one can evaluate $t_2 = 5$ as the mean value for an undistorted lattice, and $t_2 = 7.5$, 7.5, 6.5, and 7.0 for RE = Yb, Y, Er, and Dy, respectively, therefore, $t_2 = 7 \pm 1$ as the mean value for a distorted lattice. These t_2 values are similar to those determined from Table III for undistorted and distorted lattices, respectively. Concluding, the presently evaluated parameters t_2 and t_4 are equal to 7 ± 1 and -9 ± 2, respectively, for a distorted lattice in $LiREF_4(Gd^{3+})$ crystals.

6. Conclusions

The distortion consists mainly in the decrease in vertical angles of eight fluorines F^- around Gd^{3+} ion. The distortion effect can now be understood, although only five lattices of $LiREF_4$ crystals were analyzed presently. It would be very helpful to determine t_2 and t_4 parameters directly from a stress experiment.

The spin–lattice relaxation in $LiREF_4$ family of crystals does not exhibit any relation to ionic radius of RE^{3+} ions. The calculated relaxation time of $LiErF_4$ (1.0×10^{-15} s) is slightly different from those of $LiDyF_4$ (2.7×10^{-15} s) and $LiYbF_4$* (2.2×10^{-15} s). In case of different crystal families and various RE^{3+} ions, SLRT also does not differ significantly, e.g., for Gd^{3+}-doped NdF_3 crystal $\tau_1'(Nd) = 1.7 \times 10^{-15}$ s [35].

*The SLRT of Yb^{3+} calculated in [20] should be corrected to be as in present paper. The difference consists in the use of J_P in place of quantity $A_P = Z_1 Z_2 J_P$ (see Eq. (5)), where Z_1 and Z_2 are the numbers of electrons in $4f$ shell of $(4f^7)Gd^{3+}$ and $(4f^{13})Yb^{3+}$ ions, respectively. The corrected values of SLRT (Nd^{3+}) in [35] are almost contained in error bars, e.g., for the $5/2 \leftrightarrow 3/2$ transition $\tau_1'(Nd)$ is 1.73×10^{-15} s, whereas in [35] τ_1' is $(1.81 \pm 0.06) \times 10^{-15}$ s (290 K).

The author would like to express his gratitude to the referee for helpful suggestions.

References

[1] D.A. Jones, B. Cockayne, R.A. Clay, P.A. Forrester, *J. Cryst. Growth* **30**, 21 (1975).

[2] B. Cockayne, K.H. Lloyd, J.S. Abell, I.R. Harris, D.A. Jones, *J. Cryst. Growth* **36**, 205 (1976).

[3] I.A. Ivanova, A.M. Morozov, M.A. Petrova, I.G. Podkolzina, P.P. Feofilov, *Izv. Akad. Nauk SSSR, Neorgan. Mater.* **11**, 2175 (1975); *Inorg. Mater. (USA)* **11**, 1868 (1975).

[4] J. Magarino, J. Tuchendler, P. Beauvillain, I. Laursen, *Phys. Rev. B* **21**, 18 (1980).

[5] J. Tuchendler, *Phys. Rev. B* **33**, 6054 (1986).

[6] J.P. Sattler, J. Nemarich, *Phys. Rev. B* **4**, 1 (1971).

[7] P.E. Hansen, T. Johansson, R. Nevald, *Phys. Rev. B* **12**, 5315 (1975).

[8] P.E. Hansen, R. Nevald, *Phys. Rev. B* **16**, 146 (1977).

[9] C. Keller, H. Schmutz, *J. Inorg. Nucl. Chem.* **27**, 900 (1965).

[10] R.E. Thoma, G.D. Brunton, R.A. Penneman, T.K. Keenan, *Inorg. Chem.* **9**, 1096 (1970).

[11] *Gmelin Handbuch der Anorganischen Chemie Seltenerdelemente*, Teil C3, Vol. 39, H. Bergmann (Ed.), Springer-Verlag, Berlin-Heidelberg, New York 1976.

[12] L.E. Misiak, P. Mikołajczak, M. Subotowicz, *Phys. Status Solidi A* **97**, 353 (1986).

[13] *Powder Diffraction File, Inorganic Compounds*, Ed. W.F. McClune, Join Committee on Powder Diffraction Standards — International Center for Diffraction Data, Pennsylvania 1978.

[14] L.E. Misiak, S.K. Misra, P. Mikołajczak, *Phys. Rev. B* **38**, 8673 (1988).

[15] J.H. Van Vleck, *Phys. Rev.* **74**, 1168 (1948).

[16] S.K. Misra, U. Orhun, *Phys. Rev. B* **39**, 2856 (1989).

[17] T. Mitsuma, *J. Phys. Soc. Jpn.* **17**, 128 (1962).

[18] A. Abragam, B. Bleaney, *Electron Paramagnetic Resonance of Transition Ions*, Clarendon Press, Oxford 1970.

[19] P.W. Anderson, P.R. Weiss, *Rev. Mod. Phys.* **25**, 269 (1953).

[20] L.E. Misiak, S.K. Misra, U. Orhun, *Phys. Status Solidi B* **154**, 249 (1989).

[21] J. Als-Nielsen, L.M. Holmes, H.J. Guggenheim, *Phys. Rev. Lett.* **32**, 610 (1974).

[22] L.W. Xu, H.M. Crosswhite, J.P. Hessler, *J. Chem. Phys.* **81**, 698 (1984).

[23] A.K. Kupchikov, B.Z. Malkin, A.L. Natadze, A.I. Ryskin, *Sov. Phys.-Solid State (USA)* **29**, 1913 (1987) (translation of *Fiz. Tverd. Tela (USSR)* **29**, 3335 (1987)).

[24] L.E. Misiak, P. Mikołajczak, *Acta Phys. Pol.* **A75**, 621 (1989).

[25] G. Amoretti, D.C. Giori, V. Varacca, J.C. Spirlet, J. Rebizant, *Phys. Rev. B* **20**, 3573 (1979).

[26] Y. Vaills, J.Y. Buzaré, J.Y. Gesland, *Solid State Commun.* **45**, 1093 (1983).

[27] Vishwamittar, S.P. Puri, *J. Phys. C, Solid State Phys.* **7**, 1337 (1974).

[28] J. Als-Nielsen, L.M. Holmes, F. Krebs Larsen, H.J. Guggenheim, *Phys. Rev. B* **12**, 191 (1975).

[29] J. Kuriata, W. Pastusiak, *Acta Phys. Pol.* **A66**, 627 (1984).

[30] D.J. Newman, W. Urban, *Adv. Phys.* **24**, 793 (1975).

[31] Vishwamittar, S.P. Puri, *J. Chem. Phys.* **61**, 3720 (1974).

[32] S.K. Misra, P. Mikołajczak, N.R. Lewis, *Phys. Rev. B* **24**, 3729 (1981).

[33] E. Siegel, K.A. Müller, *Phys. Rev. B* **19**, 109 (1979).

[34] V.K. Sharma, *J. Chem. Phys.* **54**, 496 (1971).

[35] W. Korczak, M.L. Paradowski, L.E. Misiak, *Phys. Status Solidi B* **165**, 203 (1991).